Journal of Mechanical Research and Application JMRA
ISSN: 2251-7383, eISSN: 2251-7391
Vol. 7, No.1, 2017, 1-12

Torsion of cylindrically poroelasic circular shaft with radial inhomogeneity .some exact solutions for extruder

Mohammad Farid Khansanami[1*], Faranak Khansanami[2]

Received: 2017- 03- 14 Accepted: 2017- 04 - 03

Abstract: Torsion of elastic and poroelastic circular shaft of radially inhomogeneous, cylindrically orthotropic materials is studied with emphasis on the end effects example for extruder. To examine the conjecture of Saint-Venant's torsion, we consider torsion of circular shaft with one end fixed and the other end free on which tractions that results in a pure torque are prescribed arbitrarily over the free end surface. Exact solutions that satisfy the prescribed boundary conditions point by point over the entire boundary surfaces are derived in a unified manner for cylindrically orthotropic shafts with or without radial inhomogeneity and for their coun- terparts of Saint-Venant's torsion. Stress diffusion due to the end effect is examined in the light of the exact solutions.The present study enables us to assess Saint-Venant's principle as applied to anisotropic, non-homogeneous poroelastic bodies in general and to evaluate the stress diffusion in torsion of radially inhomogeneous, cylindrically orthotropic cylinders in particular. The following conclusions can be drawn from the analysis.

Keywords: FGM and poroelastic shaft, Radial inhomogeneity, Torsion, extruder

1. Introduction

Torsion is one of the interesting fields for researchers. In 1903, Prandtl [1] introduced the stress function of the Saint-Venant torsion and the method of membrane analogy [2]. He presented a membrane analogy for torsional analysis and proved the accuracy and efficiency of his approximation. Baron [3] studied torsion of hollow tubes by multiplying the connected cross sections. He used an iterative method to satisfy the equilibrium and compatibility equations. A computational method for calculating torsional stiffness of multi-material bars with arbitrary shape was studied by Li et Al. [4]. In this work, they considered additional compatibility and equilibrium equations in common boundaries of different materials in

*. Ph.D student, Department of Mechanical Engineering, South Tehran Branch, Islamic Azad University, Tehran, Iran (Email address: mf.khansanami@gmail.com).09356617849
2.Ms.c , Department of Engineering, Zanjan University, Zanjan, Iran (Email address: f.khansanami.arch@gmail.com)

their formulation and, good results were obtained. Mijak [5] considered a new method to design an optimum shape in beams with torsional loading. In his work, cost function was torsional rigidity of the domain and constraint was the constant area of the cross-section while shape parameters were co-ordinates of the finite element nodes along the variable boundary. The problem was directly solved by optimizing the cost function with respect to the shape parameters. He solved this problem using finite elements (FE) method. Kubo and Sezawa [6] presented a theory for calculating the torsional buckling of tubes and also reported on experimental results for rubber models. However, this theory did not conform to experimental results. Lundquist [7] performed extensive experiments on the strength of aluminum shafts under torsion reported in 1932. Recently, Doostfatemeh et al. [8] obtained a closed-form approximate formulation for torsional analysis of hollow tubes with straight and circular edges. In this work, the problem was formulated in terms of Prandtl's stress function. Also, accuracy of the formulas was verified by accurate finite element method solutions.

In recent years, the composition of several different materials has been often used in structural components in order to optimize responses of the structures subjected to thermal and mechanical loads. Since these pioneering works established the theory of torsion and solved many problems in engineering application, the torsion of a straight bar became a classical problem in the theory of elasticity, which was also presented as a numerical example in a seminal paper about the finite element method by Courant [9]. Some analytical solutions of the homogeneous section with various shapes are available in the literatures [10, 11]. The torsion of composite shafts has attracted many researchers' attention in the development and application of composite materials. Muskhelishvilli [12] presented not only the governing equation and boundary condition of the torsion of composite bars, but also its solution in Fourier series for composite section with two sub-rectangles. This solution was extended later for multiple rectangular composite section by Booker and Kitipornchai [13]. Kuo and Conway [14–17] analyzed the torsion of the composite sections of various shapes. Packham and Shail [18] extended their work on two-phase fluid to the torsion of composite shafts. Ripton [19] investigated the torsional rigidity of composite section reinforced by fibers. Chen et al. [20] also analyzed exactly the torsion of composite bars. Apart from these analytical methods, numerical methods have also been employed to solve the torsion of the straight bars. Ely and Zienkiewicz [21] firstly solved the Poisson's equation of the Prandtl's stress function using finite difference method, and then they investigated the rectangular section with and without holes. Herrmann [22] utilized the finite element method to calculate the warping function of the torsion of irregular sectional shapes. The boundary element method was applied to solve the boundary integral equation of the warping function of the torsion in Refs. [23–26].

Recently Poro's properties have been developed to overcome the problems associated with interfaces in traditional composite materials due to the abrupt change of the materials properties, as they

continuously vary with spatial coordinates [27]. Despite of less attention paid to this subject, Ely and Zienkiewicz [21] and Plunkett [28] presented the governing equation of the torsion of inhomogeneous material before the introduction of the conception of Poros, as there is no engineering significance at that time. Once the FGMs were fabricated and applied in engineering practice, Rooney and Ferrari [29,30] and Horgan and Chan [31] resumed the research on the torsion of FGM bars. More recently, Tarn and Chang [32] obtained the exact solution of the torsion of orthotropic inhomogeneous cylinders and also analyzed the end effect. In particular, the torsion problem for inhomogeneous isotropic elastic materials has been investigated recently in [33]. Poroelasticity is a theory that models the interaction of deformation and fluid flow in a fluid-saturated porous medium. The deformation of the medium influences the flow of the fluid and vice versa. The theory was proposed by Biot [34-36]. As a theoretical extension of soil consolidation models developed to calculate the settlement of structures placed on fluid-saturated porous soils, The historical development of the theory is sketched by de Boer (1996). The theory has been widely applied to geotechnical problems beyond soil consolidation that are the most notably problems in rock mechanics. There has been recently a growing interest in the context of non-homogeneous and/or anisotropic shaft. Arghavan and Hematiyan[37] analyzed the Torsion of functionally graded hollow tubes. Batra [38] ,Horgan and Chan [39] work on Torsion of a functionally graded cylinder; Rooney and Ferrari [40]; Udea et al [41] and Yaususi and Shigeyasu [42] analyzed the Torsion and flexure of inhomogeneous elements; Khansanami and Jabbari [43] work on torsion of proElastic shaft.

2. Governing Equations

Stress-Stress Function Formulation[44]

The stress formulation leads to the use of a stress function similar to the results of the plane problem discussed. Using the displacement form, the strain-displacement relations give the following strain field:

$$\boldsymbol{e}_x = \boldsymbol{e}_y = \boldsymbol{e}_z = \boldsymbol{e}_{xy} = \mathbf{O} \tag{1}$$

$$e_{xz} = \frac{1}{2}\left(\frac{\partial w}{\partial x} \quad \alpha y\right) \tag{2}$$

$$e_{yz} = \frac{1}{2}\left(\frac{\partial w}{\partial y} + \alpha x\right) \tag{3}$$

The corresponding stresses follow from Hooke's law:

$$\sigma_x = \sigma_y = \sigma_z = \tau_{xy} = 0 \tag{4}$$

$$\tau_{xz} = \mu\left(\frac{\partial w}{\partial x} \quad \alpha y\right) \tag{5}$$

$$\tau_{yz} = \mu\left(\frac{\partial w}{\partial y} + \alpha x\right) \tag{6}$$

Note that the strain and stress fields are functions only of x and y. For this case, with zero body forces, the equilibrium equations are reduced to

$$\frac{\partial \tau_{xz}}{\partial x} + \frac{\partial \tau_{yz}}{\partial y} = 0 \tag{7}$$

Rather than using the general Beltrami-Michell compatibility equations, it is more desirable to develop a special compatibility relation for this particular problem. This is easily done by simply differentiating (5) with

respect to y and (6) regarding x and subtracting the results to get

$$\frac{\partial \tau_{xz}}{\partial y} - \frac{\partial \tau_{yz}}{\partial x} = 2\mu\alpha \tag{8}$$

This represents an independent relation among the stresses developed under the continuity conditions of w(x,y).

Relations (7) and (8) constitute the governing equations for the stress formulation. The coupled system pair can be reduced by introducing a stress function approach. For this case, the stresses are represented in terms of the Prandtl stress function $\varphi = \varphi(x, y)$ by

$$\tau_{xz} = \frac{\partial \varphi}{\partial y} \tag{9}$$

$$\tau_{yz} = -\frac{\partial \varphi}{\partial x} \tag{10}$$

The equilibrium equations are then identically satisfied and the compatibility relation gives the following relation:

$$\nabla^2 \varphi = \frac{\partial^2 \varphi}{\partial x^2} + \frac{\partial^2 \varphi}{\partial y^2} = -2\mu\alpha \tag{11}$$

Thus, this single relation is the governing equation for the problem and (11) is a Poisson equation that is amenable to several analytical solution techniques.

To complete the stress formulation we now must address the boundary conditions on the problem. As previously mentioned, the lateral surface of the cylinder S is to be free of tractions, and thus

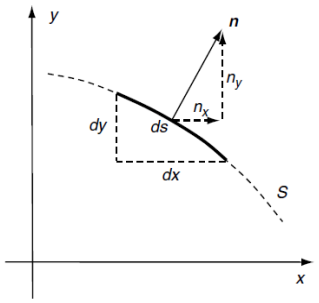

FIGURE 1 : Differential surface element.

$$\begin{aligned} T_x^n &= \sigma_x n_x + \tau_{yx} n_y + \tau_{zx} n_z = 0 \\ T_y^n &= \tau_{xy} n_x + \sigma_y n_y + \tau_{zy} n_z = 0 \\ T_z^n &= \tau_{xz} n_x + \tau_{yz} n_y + \sigma_z n_z = 0 \end{aligned} \tag{12}$$

The first two relations are identically satisfied because $\sigma_x = \sigma_y = \tau_{xy} = n_z = 0$ on S. To investigate the third relation, consider the surface element shown in Figure 1. The components of the unit normal vector can be expressed as

$$n_x = \frac{dy}{ds} = \frac{dx}{dn}, n_y = -\frac{dx}{ds} = \frac{dy}{dn} \tag{13}$$

Using this result along with (7,8) in $(12)_3$ gives:

$$\frac{\partial \varphi}{\partial x}\frac{dx}{ds} + \frac{\partial \varphi}{\partial y}\frac{dy}{ds} = 0 \tag{14}$$

which can be written as

$$\frac{d\varphi}{ds} = 0, \quad on \ S \tag{15}$$

This result indicates that the stress function φ must be a *constant* on the cross-section boundary. Because the value of this constant is not specified, we may choose any convenient value and this is normally taken to be zero. Next consider the boundary conditions on the ends of the cylinder. On this boundary, components of the unit normal

become $n_x = n_y = 0$, $n_z = \pm 1$, and thus the tractions simplify to

$$\begin{aligned} T_x^n &= \pm \tau_{xz} \\ T_y^n &= \pm \tau_{yz} \\ T_z^n &= 0 \end{aligned} \qquad (16)$$

Recall that we are only interested in satisfying the resultant end-loading conditions, and thus the resultant force should vanish while the moment should reduce to a pure torque *T* about the z-axis. These conditions are specified by

$$p_x = \int_R T_x^n \, dx \, dy = 0 \qquad (17\text{-}1)$$

$$p_y = \int_R T_y^n \, dx \, dy = 0 \qquad (17\text{-}2)$$

$$p_z = \int_R T_z^n \, dx \, dy = 0 \qquad (17\text{-}3)$$

$$M_x = \int_R y T_z^n \, dx \, dy = 0 \qquad (17\text{-}4)$$

$$M_y = \int_R x T_z^n \, dx \, dy = 0 \qquad (17\text{-}5)$$

$$M_z = \int_R (x T_y^n - y T_x^n) \, dx \, dy = T \qquad (17\text{-}6)$$

With $T_z^n = 0$, conditions (17-3 to 17-5) are automatically satisfied. Considering the first condition in set (17), the *x* component of the resultant force on the ends may be written as

$$\int_R T_x^n \, dx \, dy = \pm \int_R \tau_{xz} \, dx \, dy = \pm \int_R \frac{\partial \phi}{\partial y} \, dx \, dy \qquad (18)$$

Using Green's theorem, $\int_R \frac{\partial \phi}{\partial y} \, dx \, dy = \oint_s \phi \, n_y \, ds$ and because ϕ vanishes on boundary S , the integral is zero and the resultant force P_x vanishes. Similar arguments can be used to show that the resultant force P_y will vanish. The final end condition (17-6) involving the resultant torque can be expressed as

$$T = \int_R (x T_y^n - y T_x^n) \, dx \, dy = \int_R \left(x \frac{\partial \phi}{\partial x} + y \frac{\partial \phi}{\partial y} \right) dx \, dy \qquad (19)$$

Reapplying above equation, the following equation results from Green's theorem

$$\int_R x \frac{\partial \phi}{\partial x} \, dx \, dy = \int_R \frac{\partial}{\partial x} (x\varphi) \, dx \, dy \quad \int_R \varphi \frac{\partial x}{\partial x} \, dx \, dy = \oint_s x\varphi \, n_x \, ds \quad \int_R \varphi \frac{\partial x}{\partial x} \, dx \, dy \qquad (20\text{-}1)$$

$$\int_R y \frac{\partial \phi}{\partial y} \, dx \, dy = \int_R \frac{\partial}{\partial y} (y\varphi) \, dx \, dy \quad \int_R \varphi \frac{\partial y}{\partial y} \, dx \, dy = \oint_s y\varphi \, n_y \, ds \quad \int_R \varphi \frac{\partial y}{\partial y} \, dx \, dy \qquad (20\text{-}2)$$

Because — is zero on S, the boundary integrals in (20-1 and20-2) will vanish and relation (19) simplifies to

$$T = 2 \int_R \varphi \, dx \, dy \qquad (21)$$

3. Results and discussion

As a simple measure to estimate the stress disturbance from the end in a long circular shaft, which is the distance measured from the end beyond which the series terms contribute only 1% in magnitude to the deformation and stresses. In other words, the deformation and stresses in the region beyond *L* from the end are essentially inde- pendent of the load distribution over the end surface so that the Saint-Venant solution should be applicable. Of course, other percentage could be chosen for the estimation and the smallest eigenvalue $k1$ should be used to determine the largest *L*.

Knowing λ_{1b}= 5.1355 for a homogeneous shaft, so

$$L=\ln 100/k\lambda_1=0.8967b\sqrt{c44/c66} \qquad (22)$$

which suggests that the end effect is far-reaching for strong anisotropy ($c_{44}>>c_{66}$). Since $c_{44} = c_{66}$ for isotropic materials, L = 0.8966b, suggesting that the stress disturbance is indeed confined to a local region near the end in a long homogeneous isotropic shaft. Tables 1 and 2 show the smallest eigenvalue $\lambda 1$ associated with the parameter of the radial inhomogeneity μ, and the characteristic decay length L of long circular shafts in connection with μ and the material parameter $k=\sqrt{c44/c66}$ to show the effect of anisotropy, we take $c_{44}/ c_{66} = 1, 4, 16, 100$ for computation. All cases are admissible in that they satisfy the requirement of positive-definiteness of the strain energy. Although $c_{44}/c_{66} = 100$ appears to be uncommon in practice, the value is as-

Table 1

The smallest eigenvalue for various inhomogeneity parameters

μ	0	0.1	0.2	0.5	1.0	2.0	3.0
$\lambda 1b$	5.135	5.262	5.388	5.763	6.380	7.588	8.771

Table 2

Characteristic decay length of long circular shaft

L	Isotropic	$c_{44} = 4c_{66}$	$c_{44} = 16c_{66}$	$c_{44} = 100c_{66}$
$\mu = 0$	0.897b	1.794b	3.587b	8.967b
$\mu = 0.5$	0.799b	1.598b	3.196b	7.991b
$\mu = 1.0$	0.722b	1.447b	2.887b	7.218b

sumed in the interest of demonstrating the effect of strong anisotropy. Notably, the characteristic decay length could reach as far as 9b from the free end of a strongly orthotropic ($c_{44} = 100c_{66}$) circular shaft, not to the expectation based on Saint-Venant's conjuncture.

To examine quantitatively the Saint-Venant conjecture, we consider two types of torsional load prescribed over the end surface. Load type 1: linearly distributed load, p(r)= qr. Load type 2: tangential ring load applied at the boundary of the circular section, p(r) = 0.25qb2δ(r — b), where δ(r — b) is the Dirac-delta function. Both loading types give rise to a pure torque of the same magnitude. While the linearly distributed load is continuous over the end surface, the tangential ring load is concentrated at r = b. The influence of the radial inhomogeneity and material anisotropy are studied by taking the material parameters: μ= 0 (homogeneous material), μ = 0.5 (linearly distributed radial inhomogeneity) and μ= 1.0 (quadratically distributed radial inhomogeneity); k= 1 (c44 = c66,isotropic material),k= 0.5; 0.25; 0.1 (orthotropic materials with $c_{44} = 4c66$; $c44 = 16c_{66}$; $c_{44} = 100c_{66}$, respectively) in the computation. In all the figures presented in the following the displacement and stresses have been made dimensionless.

Fig. 1 shows the variations of μ_Θ, $\sigma\theta z$ and $\sigma r\theta$ at $r = 0.5b$ in the axial direction for cylindrically orthotropic, homogeneous shafts ($\mu = 0$) subjected to the tangential ring load (load type 2). When a homogeneous shaft is subjected to linearly distributed load (load type 1), the deformation and stress distribution are identical to those of Saint-Venant's torsion. It can be observed that the end effect is far-reaching in circular shafts with strong cylindrical orthotropy ($c_{44} = 16c_{66}$; $c44 = 100c_{66}$), whereas the stress disturbance in an isotropic shaft

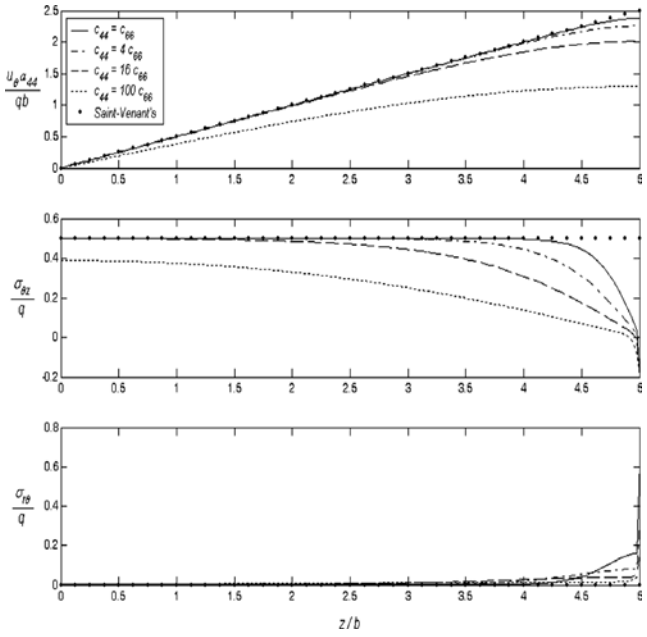

Fig. 1. Axial distribution of μ_Θ, $\sigma\theta z$ and $\sigma r\theta$ at r = 0.5b in homogeneous shafts under tangential ring load (load type 2).

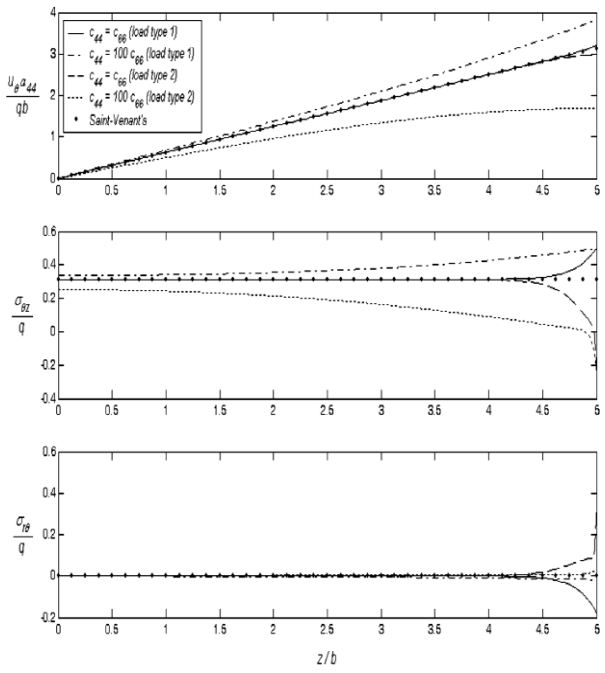

Fig. 2. Axial distribution of u_Θ, $\sigma\theta z$ and $\sigma r\theta$ at r = 0.5b in non-homogeneous shafts (μ = 0.5) under linearly distributed load (load type 1) and tangential ring load (load type 2).

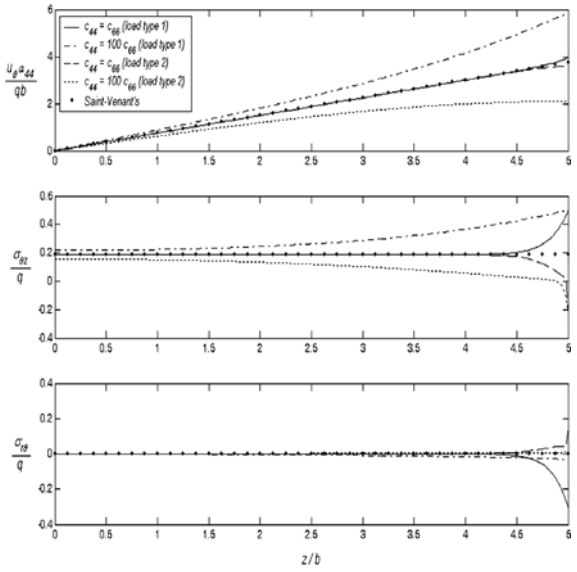

Fig. 3. Axial distribution of uΘ, σθz and σrθ at r = 0.5b in non-homogeneous shafts (μ= 1.0) under linearly distributed load (load type 1) and .(tangential ring load (load type 2

is confined to a local region near the free end. While the deviations of uΘ and σθz σθz from their Saint-Venant coun- terparts are remarkable, the end effect on σrθ is localized to the vicinity of the free end where the tangential ring load is acting.

Figs. 2 and 3 display the effects of radial inhomogeneity μ = 0.5 and μ = 1.0, in which the material is assumed to be isotropic (c44 = c66) and strongly orthotropic (c44 = 100c66), respectively. Both loading types exhibit end effects. The effect is far-reaching in the shaft with strong anisotropy subjected to the tangential ring load. The radial inhomogeneity plays a less important role in the stress distur- bance in view that the deviations from the Saint-Venant counterparts in the case of isotropy are confined to the region of a diameter from the free end for both cases of μ= 0.5 and μ = 1.0 for the reason that the characteristic decay length depends upon the smallest eigenvalue λ1 which varies slightly for different μ, as given in Table 2.

Figs. 4–7 show the radial variations of the displacement and stresses at the sections z = 0 and z = 4b in the shafts subjected to two types of torsion load with material orthotropy and radial inhomogeneity. The section z = 0 is the fixed end; the section z = 4b is chosen because it is generally expected that stress disturbance occurs within a diameter from the end according to the conjecture of Saint-Venant's torsion. The results show that at the fixed end Saint-Venant's solutions are in good agreement with the exact solution,

except for a slight difference in σθz the case of strong orthotropy under tangential ring load (Fig. 7). Surprisingly, the non-vanishing stress σθz at the fixed end does not vary significantly compared with that at z = 4b, which can be attributed to the fact that the fixed end is subjected to the same resultant torque as any other section of the circular shaft under torsion; the prescribed BC affects only the stress distribution across the section. As for the displacement and stresses at the section z = 4b, Fig. 4 reveals that the stress disturbance is confined to the vicinity near the end where the torsion load is applied; small deviation from the exact solution is observed only in σrθ. Thus Saint-Venant's conjecture is applicable to torsion of isotropic circular shafts even with radial inhomogeneity. In the case of anisotropic materials the situation is different in view of Figs. 5–

7. The stresses are greatly disturbed by the traction BC at z = 5b. As shown in Figs. 6,7, the end effect is sig-

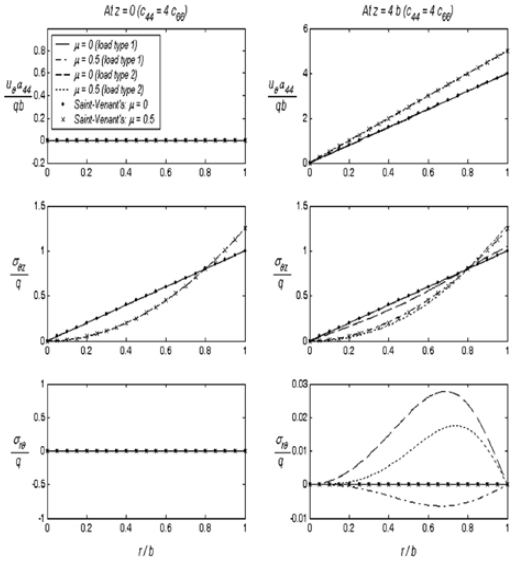

Fig. 4. Radial distribution of μθ, σθz and σrθ at z = 0; 4b in isotropic shafts under linearly distributed load (load type 1) and tangential ring load (load type 2).

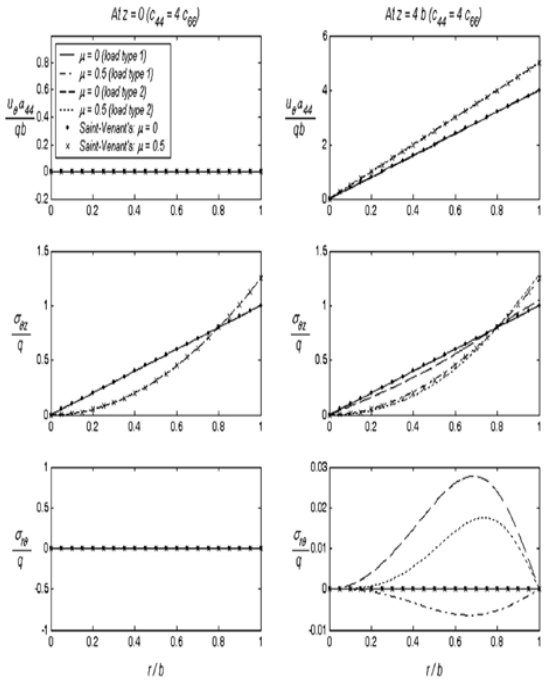

Fig. 5. Radial distribution of μΘ, σθz and σrθ at z = 0; 4b in orthotropic shafts (c44 = 4c66) under linearly distributed load (load type 1) and .(tangential ring load (load type 2

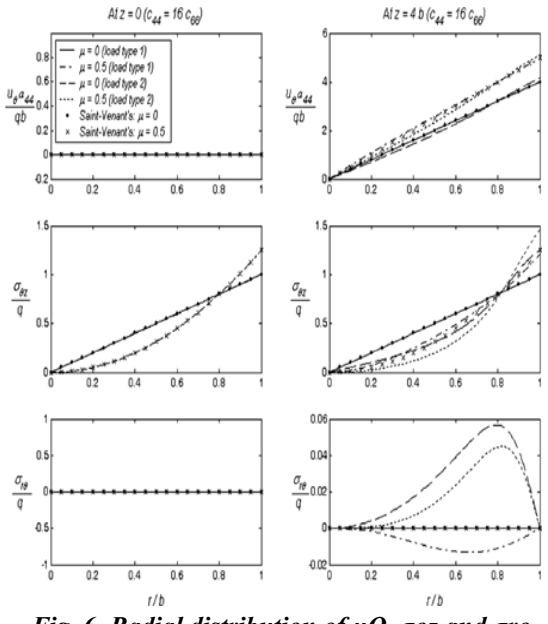

Fig. 6. Radial distribution of μΘ, σθz and σrθ at z = 0; 4b in orthotropic shafts (c44 = 16c66) under linearly distributed load (load type 1) and .(tangential ring load (load type 2

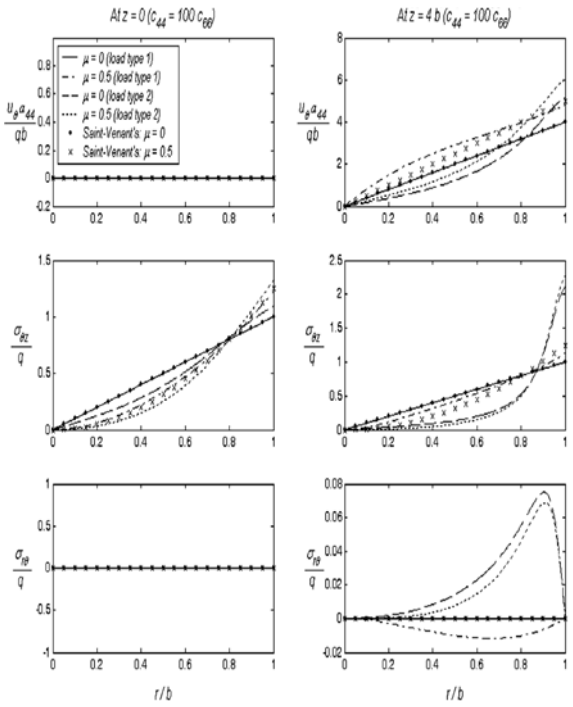

Fig. 7. Radial distribution of μΘ, σθz and σrθ at z = 0; 4b in orthotropic shafts (c44 = 100c66) under linearly distributed load (load type 1) and .(tangential ring load (load type 2

orthotropy subjected to tangential ring load. Remarkable differences exist between the exact solution and the Saint-Venant solution in which the exact traction BC are relaxed by the statically equivalent ones.

4. Conclusions

The present study enables us to assess Saint-Venant's principle as applied to anisotropic, non-homogeneous poroelastic bodies in general and to evaluate the stress diffusion in torsion of radially inhomogeneous, cylindrically orthotropic cylinders in particular. The following conclusions can be drawn from the analysis.

- The classical solution based on the Saint-Venant conjecture is useful for torsion of isotropic circular shafts with or without radial inhomogeneity. The stress disturbance is confined to the local region near the end where the torsion load is applied.
- The stresses at the fixed end of circular shafts under torsion can be evaluated using the solution based on Saint-Venant's conjecture except in the case of strong anisotropy.
- Radial inhomogeneity of the material affects the deformation and stress distribution in cylindrically orthotropic shafts, but it is not significant in evaluating the stress disturbance due to the end effect.
- The end effect is far-reaching and cannot be ignored in torsion of circular shafts with strong anisotropy. The Saint-Venant conjecture should be used with caution in such cases.

References

[1] S.-P. Timoshenko.,J.-N. Goodier , Theory of elasticity, third ed.McGraw-Hill, New York.1970.

[2] S.-P.Timoshenko., History of strength of materials, McGraw-Hill, New York.1953.

[3]F.-M.Baron, Torsion of Multi-Connected Thin-Walled Cylinders, J. Appl.1942. Mech, Vol. 9, pp. 72-74.

[4] Li.-Z.Ko, J. M. and Y.- Q. Ni, 2000,TorsionalRigidity of Reinforced Concrete Bars with Arbitrary Sectional Shape, Finite Elem. Anal .Des., Vol. 35, pp. 349-361.

[5]G.Mejak, 2000 ,Optimization of cross-section of hollow prismatic bars in torsion, Communications in Numerical Methods in Engineering, Vol. 16, pp. 687-695.

[6] K. Sezawa, K. Kubo, 1931,The buckling of a cylindrical shell under torsion, Aero Research Inst, Tokyo Imperial University, Report No. 176.

[7]E.Lundquist, 1932, Strength tests on thin-walled duralumin cylinders in torsion. NACA No. 427.

[8] A.Doostfatemeh, M.-R.Hematiyan, and S.Arghavan, 2009,Closed-form approximate formulations for torsional analyses of hollow tube with straight and circular edges, Journal of Mechanics, Vol. 25, pp. 401-409.

[9]R. Courant, 1943,Variational methods for the solution of problems of equilibrium and vibration, Bull Am Math Soc; 49(1):1–23.

[10]S.-P. Timoshenko, 1956,Strength of materials.thirded, Berkshire (England): Van Nostrand.

[11] P.-M. Quinlan, 1964,Thetorsion of an irregular polygon,Proc Royal SocLondSer A Math PhysSci; 282(1389):208–27.

[12]N.-I. Muskhelishvilli, 1953 .Some basic problems of the mathematical theory of elasticity. Groningen (Holland): P. Noordhoff.

[13]J.-R. Booker, S. Kitipornchai, 1971,Torsion of multilayered rectangular section, J EngMechDiv ASCE; 97(EM5):1451–68.

[14]Y.-M. Kuo, H.-D.Conway, 1973,The torsion of composite tubes and cylinders, I JSS; 9(12):1553–65.

[15]Y.-M. Kuo, H.-D.Conway, 1974,Torsion of cylinders with multiple reinforcement ,JEngMechDiv ASCE; 100(EM2):221–34.

[16] Y.-M. Kuo, H.-D.Conway, 1974,Torsion of composite rhombus cylinder, J ApplMech; 31(2):302–3.

[17] Y.-M. Kuo, H.-D.Conway, 1980, Torsion of reinforced square cylinder, J EngMechDiv ASCE; 106(EM6):1341–7.

[18]B.-A.Packham, R.-St. Shail, 1978 ,Venant torsion of composite cylinders, J Elasticity; 8(4):393–407.

[19] R. Ripton, 1998 ,Optimal fiber configurations for maximum torsional rigidity, Arch Ration Mech Anal; 144(1):79–106.

[20]T.Chen, Y. Benveniste, 2002, Chuang PC, Exact solutions in torsion of composite bars: thickly coated neutral inhomogeneities and composite cylinder assemblages, Proc Math PhysEngSci; 458(2023):1719–59.

[21] J.-F. Ely,O.-C.Zienkiewicz, 1960 ,Torsion of compound bars – a relaxation solution,Int J MechSci; 1(4):356–65.

[22]L.-R. Herrmann, 1965,Elastic torsional analysis of irregular shapes, J EngMechDiv ASCE (EM6):11–9.

[23] M.-A. Jaswon, A.-R., Ponter, 1963,An integral equation solution of the torsion problem,Proc Roy SocLondSer A Math PhysSci; 273(1353):237–46.

[24]J.-T.Kasikadelis, E.-J.Sapountzakis, 1986,Torsion of composite bars by boundary element method, J EngMech; 111(9):1197–210.

[25]E.-J.Sapountzakis, 2000,Solution of non-uniform torsion of bars by an integral equation method,ComputStruct; 77(6):659–67.

[26] E.-J. Sapountzakis, 2001, Nonuniform torsion of multi-material composite bars by the boundary element method, ComputStruct; 79(32):2805–16.

[27] M. Koizumi, 1993,The concept of FGM. Ceram Trans Function Grad Mater; 34(1):3–10.

[28]R., Plunkett, 1965,Torsion of inhomogeneous elastic prismatic bars, J EngInd; 87:391–2.

[29] F.-J. Rooney, M. Ferrari, 1995, Torsion and flexure of inhomogeneous elements, Compos Eng; 5(7):901–11.

[30] F.-J. Rooney, M. Ferrari, 1999, On the St. Venant problems for inhomogeneous circular bars, JApplMech; 66(2):32–44.

[31]C.-O.Horgan, A.-M.Chan, 1999,Torsion of functionally graded isotropic linearly elastic bars, J Elasticity; 52(2):181–99.

[32] J.-G. Tarn, H.-H.Chang, 2008, Torsion of cylindrically orthotropic elastic circular bars with radial inhomogeneity: some exact solutions and end effects,Int J Solids Struct; 45(1):303–19.

[33] F.-J. Rooney, M. Ferrari, 1995, Torsion and flexure of inhomogeneous elements, CompositesEngineering 5, 901–911.

[34]M.-A. Biot, 1962, Generalized theory of acoustic propagation in porous dissipative media, Journal of the Acoustical Society of America 34, 1254-1264.

[35] M.-A. Biot, 1972, Theory of finite deformation of porous solid. Indiana University Mathematics Journal 21, 597-620.

[36]M.-A.Biot, 1982, Generalized Lagrangian equations of non-linear reaction-diffusion, Chemical Physics 66, 11-26.

[37] S. Arghavan, M.-R.Hematiyan, 2009,Torsion of functionally graded hollow tubes, European Journal Mechanics A/Solids 28 (3), 551–559.

[38] R.-C. Batra, 2006,Torsion of a functionally graded cylinder, AIAA Journal 44 (6), 1363–1365.

[39] C.-O.Horgan, 2007,On the torsion of functionally graded anisotropic linearly elastic bars, IMA Journal of Applied Mathematics 72 (5), 556–562.

[40] F.-J. Rooney, M. Ferrari, 1995,Torsion and flexure of inhomogeneous elements , Composites Engineering 5 (7), 901–911.

[41] M. Udea, T. Nishimura, T. Sakate, 12–14 June 2002,Torsional analysis of functionally graded materials. In: Lao, Y.-C. Chowdhury, S.-H.Fragomeni, S. (Eds.), Advances in Mechanics of Structures and Materials: Proceedings of 17th

Australian Conference (ACMS17) .Tayor and Francis ,Queensland, Australia, pp. 533–538.

[42]T.Yaususi, A. Shigeyasu, 2000, Torsional characteristics of hemp palm branch with triangular cross-section (2-composite bar), The Japan Society of Mechanical Engineers 66 (649), 1806–1811.

[43] M.-F.Khansanami ,M. Jabbari ,Torsion of poroelastic shaft with hollow elliptical section, JSM Journal of solid Mechanics Vol.8, No.1 (2016)pp.1-11

[44] H.-sadd.Martin,2009, Elasticity theory, application and numeric, second ed .Department of mechanical engineering and applied mechanics university of Rhode Island, 229-232